applied optics

Fast template matching method in white-light scanning interferometry for 3D micro-profile measurement

Yiliang Huang,[1] Jian Gao,[1,2,*] Lanyu Zhang,[1] Haixiang Deng,[1] and Xin Chen[1,2]

[1]State Key Laboratory of Precision Electronic Manufacturing Equipment and Technology, Guangdong University of Technology, Guangzhou 510006, China
[2]Key Laboratory of Intelligent Detection and The Internet of Things In Manufacturing, Ministry of Education, Guangdong University of Technology, Guangzhou 510006, China
*Corresponding author: gaojian@gdut.edu.cn

Received 9 October 2019; revised 13 December 2019; accepted 13 December 2019; posted 16 December 2019 (Doc. ID 379996); published 28 January 2020

White-light scanning interferometry (WLSI) is an important measurement technique that has been widely used in three-dimensional profile reconstruction. Because of the effects of environmental noise and phase changes caused by surface reflection, existing WLSI algorithms have problems in measurement accuracy and measurement speed. Addressing these problems, this paper proposes a fast template matching method to determine precisely the zero optical path difference (ZOPD) position in the WLSI. Due to the uniform shape of the interference signals, a template interference signal can be obtained in advance by performing a least-square fitting or Fourier interpolation on an interference signal of one pixel. In the method, the ZOPD position is initially obtained by the centroid method. Then, the ZOPD position is determined by a precise matching process through moving the template interference signal on the measured interference signal. Through the two-step processes, the ZOPD position can be obtained precisely with much less time. The method was simulated and verified through the measurement of a spherical surface, a 1.8-μm-height standard step and a flip-chip substrate. The experimental results show that the proposed algorithm can achieve both high precision and fast measurement.

https://doi.org/10.1364/AO.379996

1. INTRODUCTION

White-light scanning interferometry (WLSI) is a popular technique for three-dimensional (3D) profile measurement of microscopic structures. Based on the short coherence length of the white-light source, WLSI not only inherits the noncontact, whole-field, high-accuracy characteristics of monochromatic interferometry but also solves the phase ambiguity problem of monochromatic interferometry when the measured surface discontinuous height jump exceeds a quarter wavelength [1,2]. Because of its advantages, WLSI has been widely used to measure microelectromechanical systems, semiconductors, transparent films, etc. [3–5]. In WLSI, an important concept is the position of the interference intensity maximum, called the zero optical path difference (ZOPD) position, which is closely related to the surface height information of the object. In other words, by searching the ZOPD position, a 3D surface microscopic profile of the object can be reconstructed.

The accuracy of WLSI is mainly determined by the location accuracy of the ZOPD position, which is generally obtained by a white-light interference processing algorithm. So far, much effort has been made to develop various algorithms. Generally, these algorithms can be classified into two groups. The first one is to seek the ZOPD position through introducing the phase method, such as white-light phase-shifting interferometry (WLPSI) methods [6], windowed Fourier transform [7,8], spatial frequency domain analysis [9], and continuous wavelet transform [10]. The second one is to identify the peak position of the white-light interference signal envelope, such as the centroid method [11,12], Fourier transform method [13], and Hilbert transform method [14]. The WLPSI method, developed from the phase-shifting interferometry method, calculates the maximum modulation point to locate zero-order fringes and then calculates the phase value to obtain the ZOPD position. This method can solve the problem of phase ambiguity, but may have the problem of locating error of the maximum modulation. This is because it takes only five sample points into account, which is easily affected by environmental vibration, and assumes the scanning step is 90° phase shift [15]. In addition, the WLPSI method requires calibration of the center wavelength of the system source, which will introduce calibration error and affect the final accuracy of the algorithm. The algorithm based on the

windowed Fourier transform [8] can achieve high-precision measurement though extracting the phase of a white-light interferogram and compensating for the difference in ZOPD position. These mentioned methods, for example, the windowed Fourier transform method [8], the continuous wavelet transform method [10], the Fourier transform method [13], and the spatial frequency domain method [9], may have strong anti-noise ability and achieve a high measuring accuracy. However, they require large amount of calculation and they are time-consuming for the measurement. The centroid method can realize a fast measurement, but it has a poor anti-interference capability and low measuring accuracy [16].

Currently, there exists a different approach to determinate the ZOPD position. When the WLSI system light source and the numerical aperture of the objective lens are determined and a well-aligned plane specularly reflecting surface is assumed, the shape of the white-light interference signal is nearly uniform for each pixel. The only difference is the ZOPD position, which is varied with the height of the object to be measured. Therefore, the interference signal can be acquired in advance and used as a template interference signal later for the match of the ZOPD position. Similar ideas have been mentioned in one way or another by some researchers [17–21]. These studies still have certain limitations either in measuring objects or efficiency. The methods in [17,18] were used to measure transparent films with a complex window selection and a least-square fitting. The studies in [19,20] utilized the correlogram correlation (CorCor) method to calculate the relative displacement of interference signal between different pixels, which can effectively eliminate the influence of the source spectrum and achieve an accurate profile measurement. The work in [21] used a complex correlation to determine the surface height with a normal resolution and reduced the noise level by using the underlying carrier fringes in the interference pattern. However, these cross-correlation method may result in an efficiency problem. The works in [19,20] involved the calculation of frequency domain cross-correlation functions and multiple Fourier interpolation, while the work in [21] involved the complex operation, Fourier transform, and inverse transform, etc. Therefore, it is necessary to find a capable method of achieving high-precision and high-efficiency ZOPD location for the surface topography reconstruction.

In this paper, we propose a template matching method to identify the ZOPD location precisely with much less time. For the measurement system, the shape of the interference signal for each pixel is similar and stable. So, the interference signal can be used as a template to precisely define the ZOPD location, which can be obtained by performing a template function fitting or Fourier interpolation on the interference signal of one pixel in the measurement. Based on the template interference signal, we can obtain the ZOPD positioning through a fast template matching (FTM) process. In order to achieve a fast match, the ZOPD position is coarsely determined through the centroid method [11,12], and then the ZOPD position is precisely determined through the template matching of the interference signal. In this way, the ZOPD position can be accurately identified with much less time and the 3D surface microscopic profile can thus be reconstructed with high precision.

2. PRINCIPLE OF THE METHOD

A. Principle of White-Light Scanning Interferometry

Figure 1 shows a schematic of a typical Mirau WLSI system, which is mainly composed of an illumination system, an optical system, a CCD camera, a piezoelectric transducer (PZT) nanopositioning stage, and a computer. The lighting system adopts a white-light source with a continuous wide spectrum. The optical system is a Mirau-type interferometric microscope. The white light passes through the collimating lens and the Mirau-type interference objective comprising a beam splitter, which divides the original light beam into a reference and an object beam. The reference beam reflected from the reference mirror is recombined with the objective beam reflected from the surface of the test object, and an interference pattern forms if the optical path difference between the two is within the coherence length of the illumination source. In particular, when the optical path difference between the reference beam and object beam is equal to zero, the intensity maximum of the interference signal, the ZOPD position, can be observed. The CCD camera records a series of interference patterns when the PZT stage controlled by the controller scans along the z-direction, and the interference signal of each pixel can be obtained, as shown in Fig. 2. Through the analysis of the interference signal, the ZOPD position of each pixel can be determined, and thus the 3D profile of the measured object can be reconstructed.

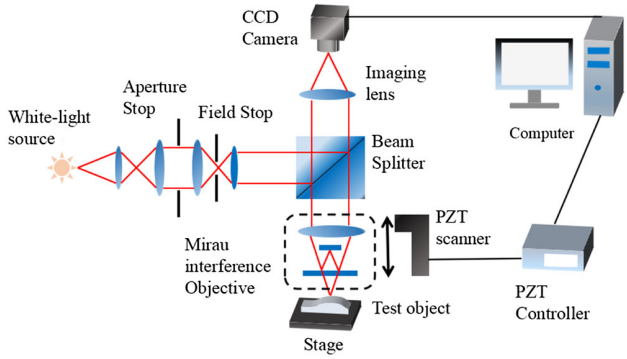

Fig. 1. Schematic of the WLSI system.

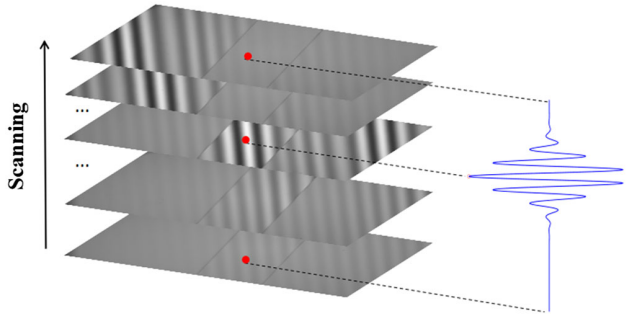

Fig. 2. Schematic of WLSI interference patterns and interference signal.

B. Principle of the Fast Template Matching Method

1. Preparation of the Template Interference Signal

The intensity function of the interference signal can be described as [20]

$$I(z) = I_b\left\{1+\gamma\exp\left\{-\left(\frac{z-z_0}{l_c}\right)^2\right\}\cos\left[\frac{4\pi}{\lambda_0}(z-z_0)+\alpha\right]\right\}, \tag{1}$$

where I_b is the background intensity; γ is the modulation; l_c and λ_0 represent the coherence length and the center wavelength of the white-light source, respectively; z denotes the vertical scanning axis; and peak position z_0 of the coherence envelope indicates the height of the measured object. α is the phase change on reflection depending on surface materials, source wavelength, and N.A. value of the objective. According to the intensity function, once the white-light source, surface materials, and N.A. value of the objective are determined, the intensity distribution of the interference signal can be estimated. The interference signals of all pixels can be considered the same, except for position z_0. As a result, an interference signal of one pixel can be acquired in advance as a template interference signal, and then the interference signal of each pixel can be matched with it to find the ZOPD position. However, in this case, the accuracy of the matching is limited by the discreteness of the sampling points, so it is necessary to obtain a nearly continuous template interference signal, i.e., a higher-resolution grid.

There are two ways to obtain the nearly continuous template interference signal. For the discrete sampling sequence of one pixel obtained in advance, the first way is to obtain the template interference signal by least-square fitting, while the second way is to use the Fourier interpolation (see MATLAB function interpft). For the first way, according to Eq. (1), γ, z_0, l_c, λ_0, and α can be obtained by fitting, and I_b can be obtained from the first image without the interference fringe, so that the exact expression of the template interference signal is determined. Because the spectral distribution of the source may not be a Gaussian distribution, such as the distribution of a white-light LED source, then it may use other suitable expression for a more accurate fitting, instead of Eq. (1). The second method can overcome such a problem, and the high-resolution template interference signal can be obtained by performing Fourier interpolation on interference signal. Thus, in this study, the second way was adopted and applied in the experimental test discussed later.

2. Rough Location of ZOPD Position by the Centroid Method

To speed up the template matching process, we first locate roughly the ZOPD position with a fast calculation through the centroid method [11,12]. The rough position N_0 can be calculated as

$$N_0 = \frac{\sum_{i=2}^{M} z_i[I(z_i)-I(z_{i-1})]^2}{\sum_{i=2}^{M}[I(z_i)-I(z_{i-1})]^2}, \tag{2}$$

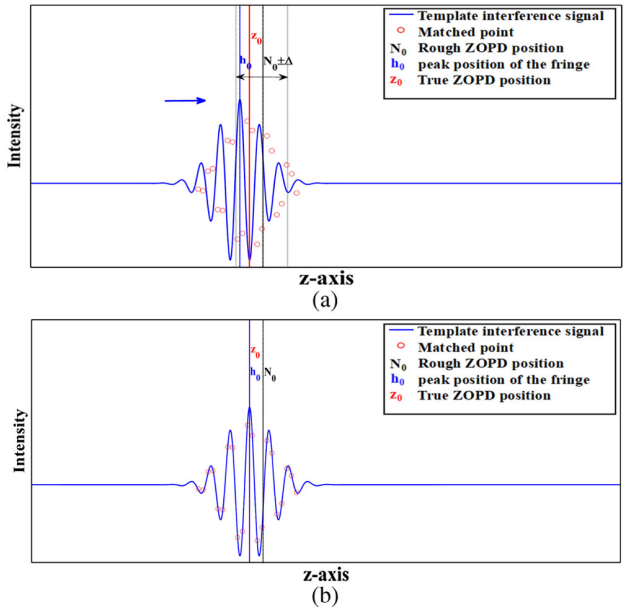

Fig. 3. Determination of the ZOPD position z_0 through the proposed method: (a) rough ZOPD position at N_0 with a searching area $N_0 \pm \Delta$, (b) precise ZOPD position at h_0.

where z_i is the discrete sampling position, and M is the number of sampling points. Then, a small search scope is chosen and denoted as $N_0 \pm \Delta$, and a small part of sample points around N_0 are chosen as matching points, as shown in Fig. 3(a).

3. Precise Determination of ZOPD Position Through the Template Matching

Considering the complete template interference signal as a whole, it can be moved along the z axis to match the sample interference signal within the search scope. The absolute value of the residual sum between the template interference signal and sample interference signal is used as an indicator for evaluating the matching accuracy:

$$\varepsilon(h_0) = \sum |I^{h_0}_{\text{template}}(z) - I_{\text{sample}}(z)|, \tag{3}$$

where the h_0 is the z-axis position corresponding to the peak value of the template signal, which represents the ZOPD position of the template interference signal. $I^{h_0}_{\text{template}}(z)$ is the intensity of the template interference signal with h_0 as the peak position. $I_{\text{sample}}(z)$ is the intensity of the sample interference signal.

Then, the best match is obtained when the $\varepsilon(h_0)$ is minimized:

$$z_0 = \arg\min_{h_0} \varepsilon(h_0). \tag{4}$$

So, the value z_0, corresponding to h_0 on the z axis, is the accurate ZOPD position of the sampled interference signal, as shown in Fig. 3(b). Thus, the corresponding height information of the measured object is also obtained.

In addition, some important details concerning the usage of the FTM method are supplemented as follows.

(1) Aiming to choose the value of Δ, if the environment noise is large, a larger value is chosen to ensure accuracy, whereas, if the environment noise is low, a smaller value is selected for higher speed. The same is true for the choice of the number of the matched points, but it should not be too small, or it will lead to information loss of the interference signal. In practice, the matched points contain at least three fringes information.

(2) The moving step of h_0, denoted as Δh_0, is an important parameter that affects the speed and accuracy of the method. If a small Δh_0 is chosen to obtain high accuracy, the template interference signal moves along the z axis slowly, which is a resource-consuming procedure. To speed up the procedure, it can be divided into two steps: rough matching and precise matching. First, the template interference signal can be moved with a larger step Δh_0 in the 2Δ range to calculate a rough matching position. Second, it can be moved with a smaller step near the coarse matching position to obtain a more accurate matching position.

(3) Due to factors such as experimental ambient light and material inhomogeneity, the offset intensity of the interference signal of each pixel may be different, which will affect the accuracy of matching. In order to remove the influence of the offset intensity, the DC components of the template interference signal and that of the measurement interference signal need to be removed before matching. The removal method is by subtracting their own average intensity of the interference signals.

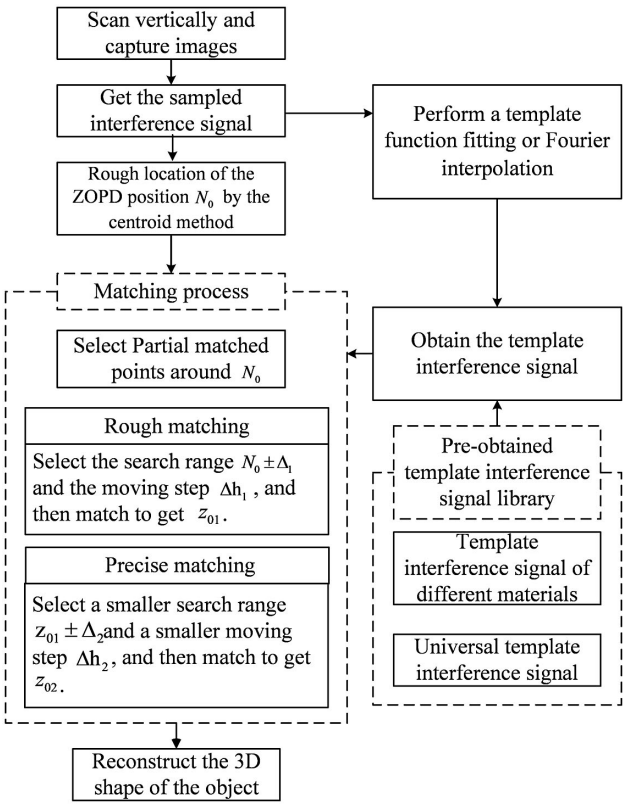

Fig. 4. Flow chart of the proposed FTM method.

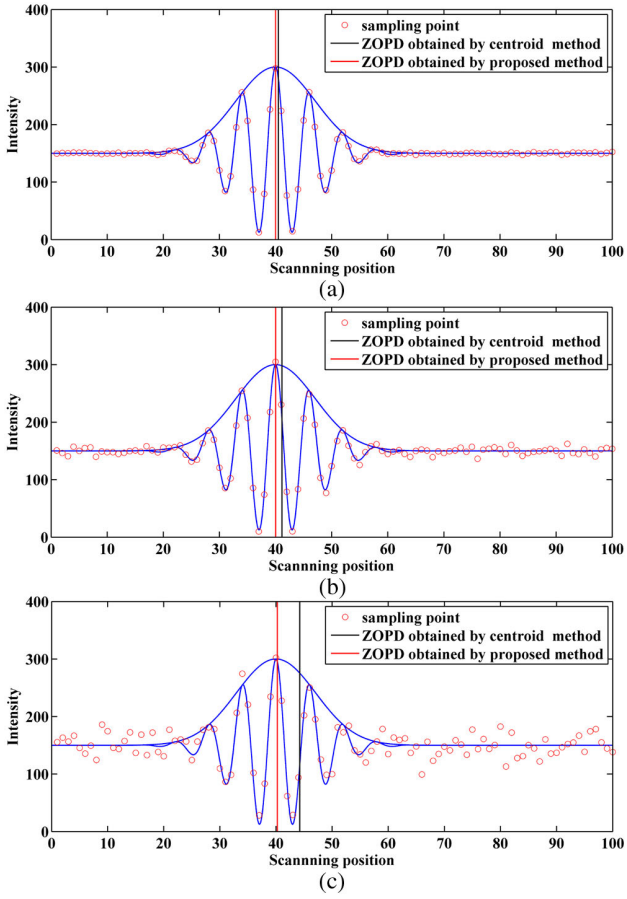

Fig. 5. Locating the ZOPD position of the interference signal with the Gaussian noise at signal-to-noise ratios of (a) 40 dB, (b) 30 dB, and (c) 20 dB by the centroid approach and the FTM method.

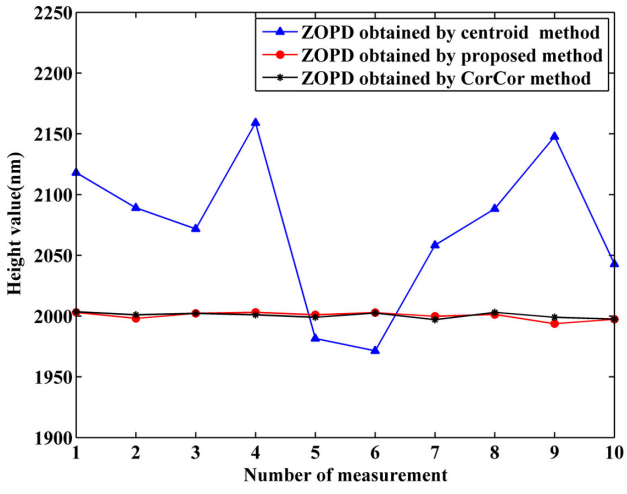

Fig. 6. Results of the height value of simulated white-light interferometry signal with 20 dB SNR Gaussian noise.

(4) If the material of the measured object changes, the phase of the interference signal will change because of the difference of its surface reflectance, so that the shape of the interference signal will be different. Therefore, using the

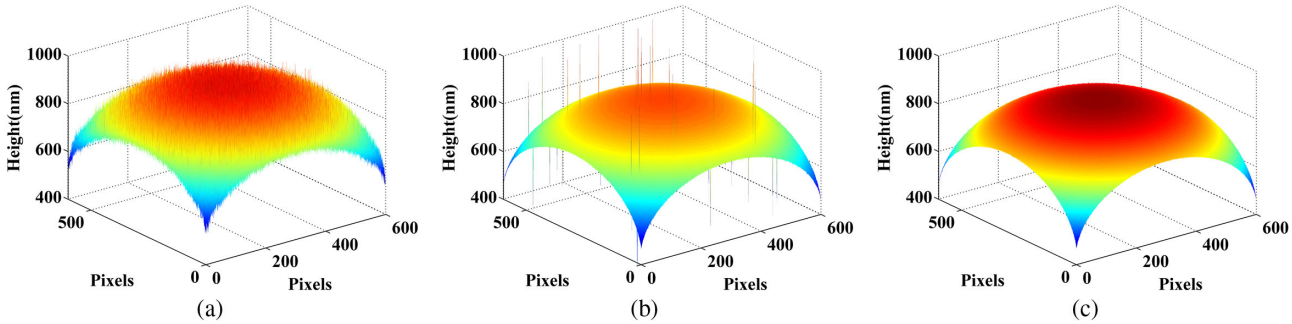

Fig. 7. 3D reconstruction of spherical surface using three different methods: (a) centroid method, (b) WLPSI method, and (c) the proposed FTM method.

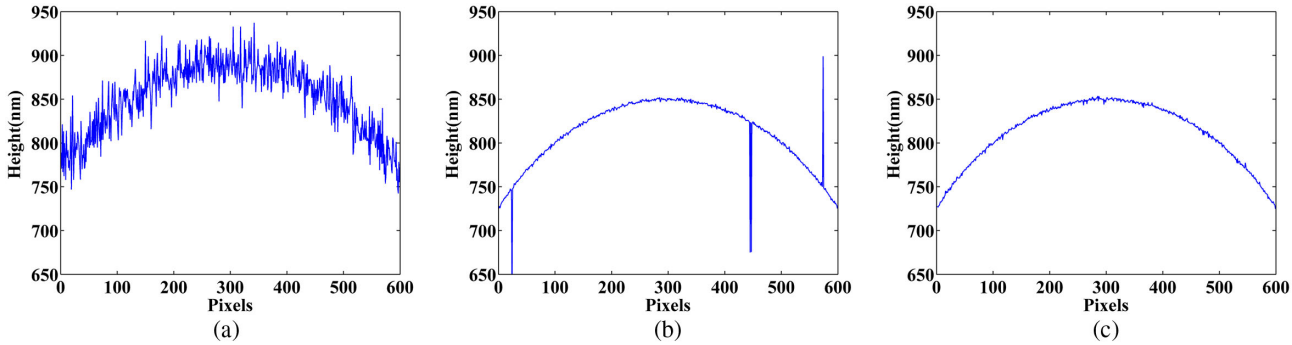

Fig. 8. Cross section of spherical surface using three different methods: (a) centroid method, (b) WLPSI method, and (c) the proposed FTM method.

same template interference signal to measure other material objects will introduce errors. This can be solved in the following three ways. (1) The first way is to recreate the template interference signal of the current measurement material. (2) The second way is to preproduce different template interference signals of different materials and select a corresponding template interference signal according to the measurement materials during measurement. (3) When the template interference signal is obtained by the least-square fitting method, the α value can be set to 0 in Eq. (1)—that is, the phase change caused by the surface reflection of the material is ignored. This can be used as a general template interference signal for different material measurement objects. Since the interference signal of the material may not be completely the same as the template used, it may affect the accuracy of the proposed algorithm.

The flow chart of the whole algorithm is shown in Fig. 4.

3. SIMULATION ANALYSIS

To verify the measuring performance of the proposed method, numerical simulation was performed. First, the generated white-light interference signal of one pixel is represented as follows:

$$I(n) = 150 + 150\exp\left[-\frac{(n-40)\Delta z^2}{\sigma^2}\right] \times \cos\left[\frac{4\pi}{\lambda_0}(n-40)\Delta z + \alpha\right], \quad (5)$$

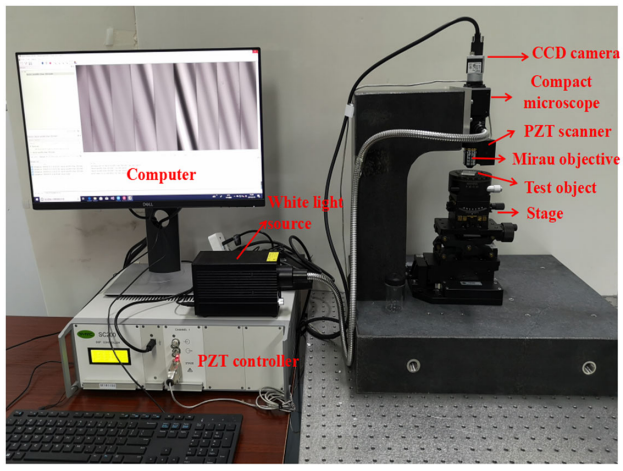

Fig. 9. Experimental arrangement for WLSI measurement.

where the σ is set to be 450 nm ($\sigma = l_c/2\pi$), the scanning step Δz is set to 50 nm, and the center wavelength of the white-light source and addition phase change are set as $\lambda_0 = 600$ nm, $\alpha = 0$. Therefore, the true location of the envelope peak of the simulated interference signal is located at $n = 40$, and the true height value is 2000 nm.

As shown in Fig. 5, three different interference signals were simulated using Eq. (5), with Gaussian noise restricted to signal-to-noise ratios (SNRs) of 40 dB, 30 dB, and 20 dB for a scanning increment of 50 nm. The SNR is defined as $10\log_{10}(P_s/P_n)$, where P_s is the signal power and P_n is the noise power (see

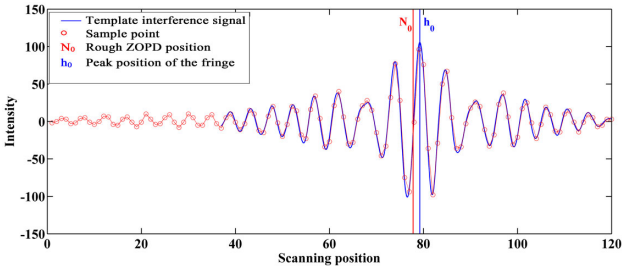

Fig. 10. Determination of the ZOPD position through the proposed method.

MATLAB function awgn). Figure 5 shows that the ZOPD position determined by the centroid method deviates farther from the true envelope peak as the SNR decreases, while the FTM method can always maintain the ZOPD position with high precision. In addition, a white-light interferometry signal with 20 dB SNR Gaussian noise was simulated and the results of the height calculated by three methods are shown in Fig. 6. It can be seen that the height values obtained by the proposed FTM method are very close to that of the CorCor method and more accurate and stable than that of the centroid approach.

For further analysis, a profile of a spherical surface with 5% random noise of the maximum fringe intensity was generated. Three algorithms were used to reconstruct the 3D spherical surface profile. The 3D reconstruction results are shown in Fig. 7 and the corresponding cross section is shown in Fig. 8. As shown in Fig. 8(a), the surface shows a noisy profile when the centroid approach is used. Figure 8(b) shows the discontinuity in some areas of the surface reconstructed by the WLPSI method. The reason is that WLPSI does not determine the exact maximum fringe modulation position, which subsequently leads to large errors. It can be seen that the proposed FTM method reconstructs a smooth surface with a high accuracy, which verifies the effectiveness of the proposed FTM method.

4. EXPERIMENTAL RESULTS AND DISCUSSION

To verify the simulated results obtained using the proposed algorithm, a WLSI 3D measurement system was developed, as

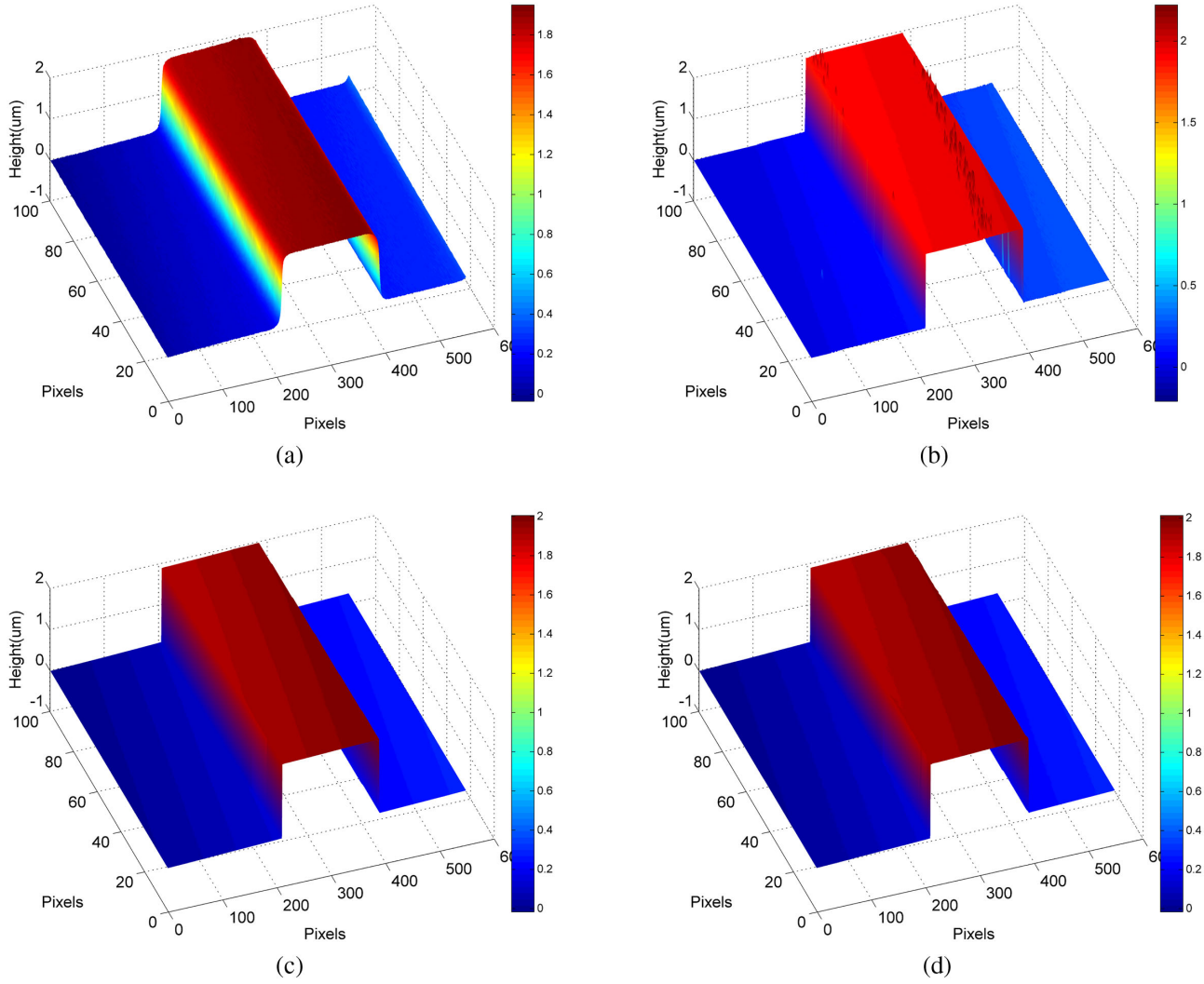

Fig. 11. 3D structure of the 1.8 μm standard height step using different methods: (a) centroid method, (b) WLPSI method, (c) CorCor method, and (d) the proposed method.

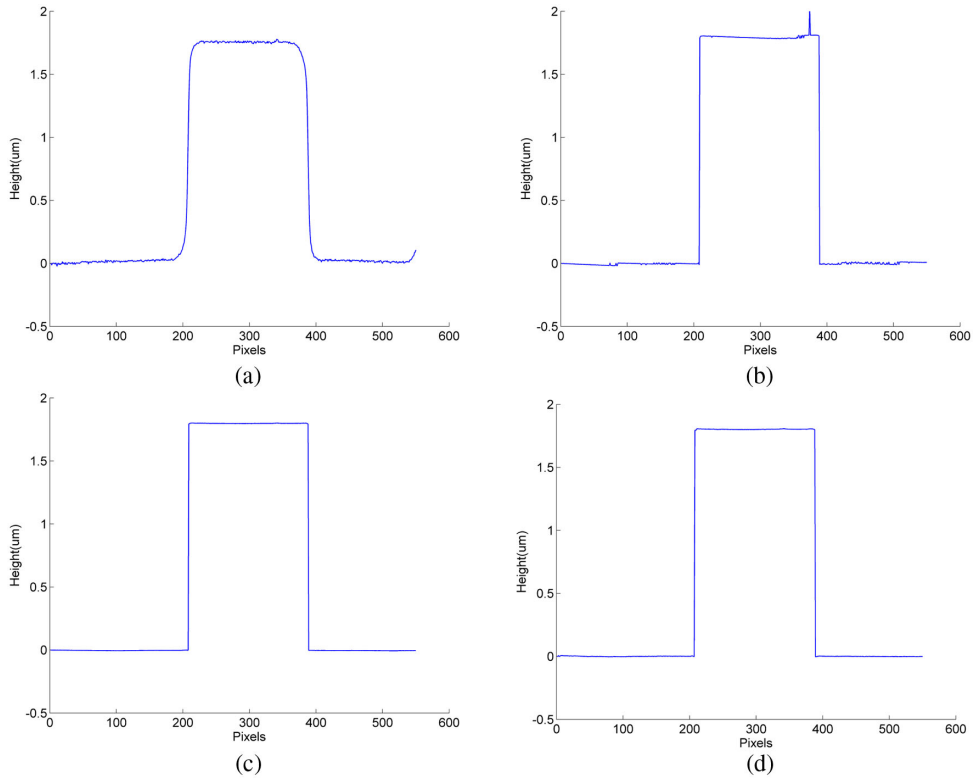

Fig. 12. Cross-section profile of the 1.8 μm standard height step using different methods: (a) centroid method, (b) WLPSI method, (c) CorCor method, and (d) the proposed method.

shown in Fig. 9. The optical system was composed of a compact microscope (Nikon, CM-30A2, Japan) and a Mirau-type interferometric microscope with an objective lens with a magnification of 10× and a numerical aperture of 0.3 (Nikon, CF IC EPI Plan DI, Japan). A PZT nanopositioning stage (SYMC, NS-Z100-02, China), controlled by the controller (SYMC, SC-200, China), was utilized to achieve the vertical scanning. For each scanning increment, the CCD camera (Sony, cA1920-155um-Baslerace, Japan) recorded the interference pattern and stored it in a computer with an Intel Core i7-8700 central processing unit (3.20 GHz and 8.00 GB of memory). The lighting system used a white-light LED source with a continuous wide spectrum, and the central wavelength was calibrated as 510 nm.

First, in order to verify the validity of the proposed method, a sample interference signal of one pixel was obtained. As is shown in Fig. 10, the rough ZOPD position is obtained through the centroid method, then the sample interference signal can be matched with the template interference signal well, and the ZOPD position is determined precisely. Then, to compare the proposed FTM method with the centroid method, WLPSI, and CorCor method, the above-described WLSI system was used to measure a standard height step of 1.8 μm, manufactured by VLSI Standards Inc. The PZT scanning increment was set to 50 nm. The 3D reconstruction surface results obtained by the four methods are shown in Fig. 11, and the corresponding cross section is shown in Fig. 12. In Fig. 11(a), the original plane surface of standard height step becomes an obviously rough surface, affected by environmental noise. Figure 11(b) shows

Table 1. Measurement Results of the 1.8 μm Standard Height Step (unit: nm)

Measurement Results	Measurement Test									
	1	2	3	4	5	6	7	8	9	10
Measurement error	1.23	1.61	−0.24	2.82	2.30	4.05	2.52	2.75	2.23	3.36
Average error	2.26									
Standard deviation	1.19									

that there are some discontinuities in the surface, which means measurement errors. The reason is that the WLPSI calculates an incorrect maximum fringe modulation position, which is not within the zero-order fringe. As shown in Figs. 11(c) and 11(d), the surface is both very continuous and smooth. However, the proposed FTM method is much faster than the CorCor method, which is shown later. It can be more clearly seen from Fig. 12 that the proposed FTM method and the CorCor method are more accurate than the centroid method and WLPSI method.

In addition, the mean value and standard deviation of 10-times measurement results are shown in Tables 1 and 2. The evaluation method of height is to fit the data of the upper and lower surface of the step cross section. As shown in Table 1, the mean height value is 1802.26 nm, and the standard deviation is 1.19 nm. This result indicates that the proposed FTM method is accurate, which is in good agreement with the standard height value. Table 2 is the comparison measurement results of the

Table 2. Comparison of Measurement Results for the 1.8 μm Standard Height Step

Measurement Results	Centroid Method	WLPSI Method	CorCor Method	Proposed Method
Mean value (nm)	1711.37	1805.19	1802.24	1802.26
Absolute error (nm)	88.63	5.19	2.24	2.26
Standard deviation (nm)	12.98	5.04	0.98	1.19
Calculation time (s)	0.33	0.81	9.46	1.08

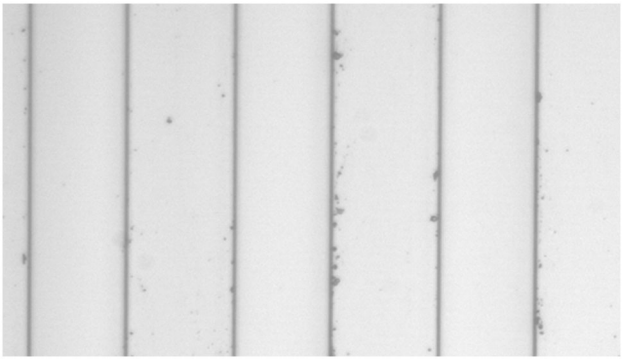

Fig. 13. Captured image of the standard multi-step.

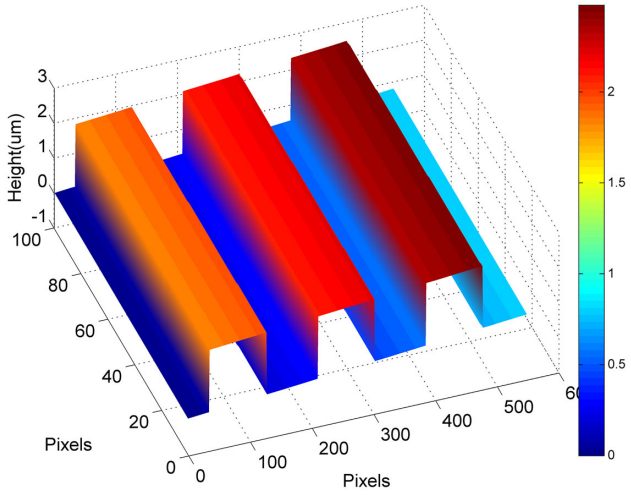

Fig. 14. 3D plot of the reconstructed standard multi-step.

standard height step by using the four methods. As shown in Table 2, the absolute errors calculated by the centroid method, WLPSI method, CorCor method, and proposed method are 88.63, 5.19, 2.24, and 2.26 nm, respectively, while the standard deviations are 12.98, 5.04, 0.98, and 1.19 nm, respectively. Therefore, the measurement accuracy and the repeatability of the proposed FTM method are better than that of the centroid method, WLPSI, and close to the CorCor method. Nevertheless, the calculation time of the proposed method is 1.08 s, while that of the CorCor method is 9.46 s. That is to say, the speed of the reconstruction using the proposed method is much faster than that of the CorCor method.

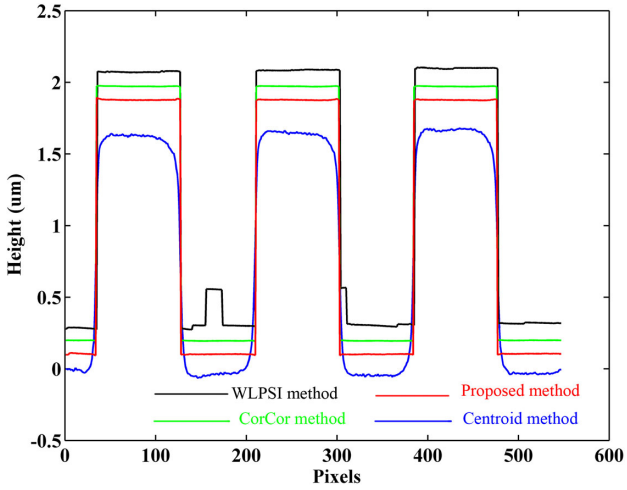

Fig. 15. Comparison of the cross sections of the standard multi-step obtained by the four methods.

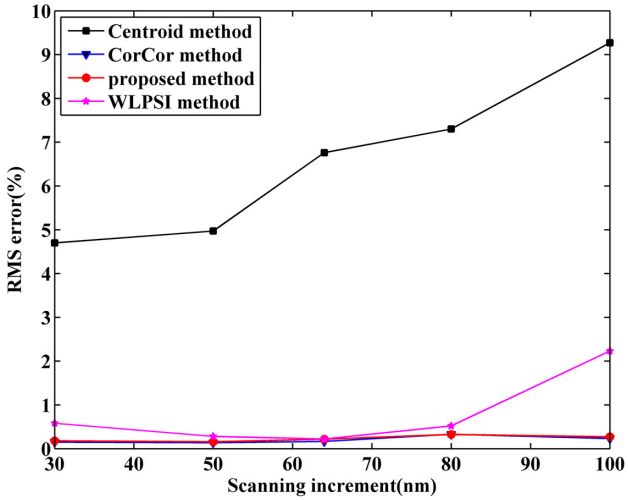

Fig. 16. Comparison of RMS error of the 1.8 μm standard height step measurement with different scanning increment.

To verify the validity of the proposed method further, a standard multi-step was scanned and evaluated using the proposed WLSI measurement system. Figure 13 shows the top view of the standard multi-step, and Fig. 14 shows the reconstructed 3D plot of the structure by the proposed method. It can be seen that the standard multi-step surface is accurately reconstructed, and the edges of the steps are very clear. For comparison, the four methods are used to reconstruct the standard multi-step surface, and the result is shown in Fig. 15. To distinguish between the sections, the curves are separated by a shift of 0.1 0.1 μm in the vertical direction. It can be clearly seen that the profile retrieved by the centroid method is rough, and there are some measurement errors on the profile with the WLPSI method, while profiles reconstructed by the proposed method and the CorCor method are smooth and accurate. As described earlier, the proposed FTM method is much faster than the CorCor method.

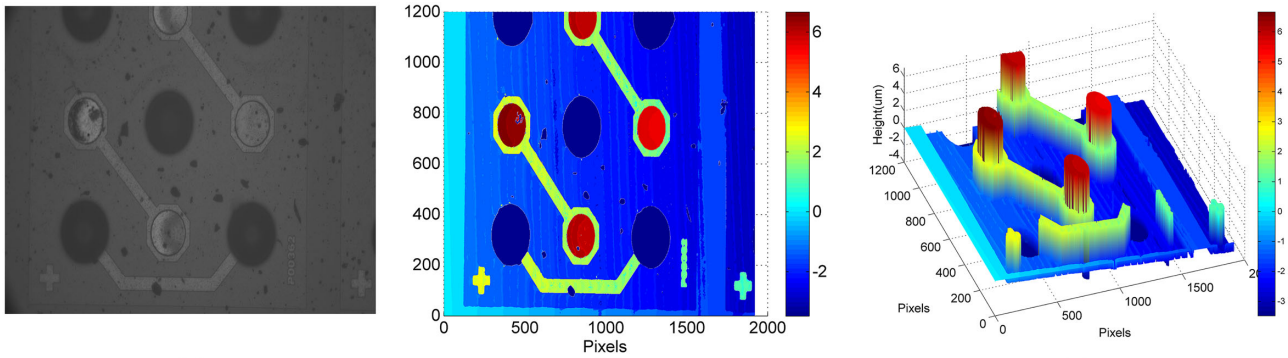

(a) (b) (c)

Fig. 17. Measurement of the flip-chip substrate using the proposed method: (a) captured image, (b) depth map, and (c) reconstructed 3D structure.

In addition, the scanning increment is an important parameter in the WLSI system, which directly affects the scanning time and reconstruction accuracy. Thus, to study the influence of different scanning increments on various algorithms, experiments were performed with increments of 30, 50, $64(\lambda_0/8)$, 80, and 100 nm. The relationship between the root-mean-square (RMS) error and the scanning increment is shown in Fig. 16. It can be seen that the proposed method has a stable, small RMS error when the scanning interval increases. This indicates that the proposed method can maintain a high accuracy with a large scanning increment satisfying the sampling theorem, and thus reducing the scanning time. The RMS error of the WLPSI method increases when the scanning increment deviates 64 nm. This is because the five-step WLPSI method requires the scanning step to be equal to $\lambda_0/8$ in theory, but the proposed method does not suffer from this problem. Finally, a flip-chip substrate was measured using the proposed method, as is shown in Fig. 17. Figure 17(a) is the captured image of the flip-chip substrate, containing some defects and dirt on the surface. Figures 17(b) and 17(c) are respectively the depth map and 3D structure of the substrate reconstructed by the proposed method. It can be seen that the surface topography and defects of the substrate are accurately reconstructed, which proves the effectiveness of the proposed method. The experimental results prove that the proposed method can achieve high precision and fast 3D reconstruction.

Since the algorithm is based on the assumption that the shape of the white-light interference signal of all pixels can be considered the same, the proposed algorithm is appropriate for the measurement of a surface with the same material, especially for specimens such as flat mirror-like surfaces or surfaces with different height plateaus. For some surfaces with multiple materials, matching the interference signals of all pixels with the same template interference signal may introduce some errors. For this case, the template interference signals of different materials can be prepared in advance, and then the plurality of template interference signals are respectively matched with the measurement interference signals. The z_0 value corresponding to the result with the smallest error among all the template matching results is taken as the final ZOPD position. For some complex surfaces, the white-light interference signal may be greatly influenced by surface reflectivity. For example, due to the influence of material inhomogeneity, roughness, local surface tilt, curvature, edge effects and other factors, the shapes of white-light interference signals at different pixels are different, which may lead to the uncertainty error of the proposed algorithm. In addition, for nontraditional test objects, such as additive manufacturing parts, aspherical or freeform lenses with highly sloped surfaces, the proposed algorithm may not work properly, which is also a challenge for white-light interferometry [22,23]. Certainly, further research is needed for the measurement of these complex surfaces or nontraditional test objects.

5. CONCLUSION

In this paper, we propose a fast template matching method in white-light scanning interferometry for 3D micro-profile measurement. The method utilizes a two-step process to initially obtain the ZOPD position quickly by the centroid method and then precisely determine the position through the template signal matching method. It can therefore determine the ZOPD position with high precision and less time. The simulation results show that the proposed method has better anti-interference ability and higher precision than the centroid method and WLPSI, and it does not suffer from 2π ambiguity. A Mirau-type interferometric microscope system was set up and used to measure a 1.8 μm standard height step. Compared with four different methods, the experimental results demonstrate that the proposed method can achieve a higher measuring accuracy than that of the centroid method and WLPSI method, and its measuring accuracy is close to that of the CorCor method, but the measuring speed is much faster than that of the CorCor method. Furthermore, the proposed method can maintain a stable measuring accuracy even in a large scanning increment so that it can reduce scanning time. Therefore, the proposed method is an effective method for the white-light interferometry.

Funding. National Natural Science Foundation of China (51675106, 61705045, U1601202); Guangdong Provincial Applied Science and Technology Research and Development Program (2016A030308016, 2018B090906002).

Disclosures. The authors declare no conflicts of interest.

REFERENCES

1. I. Shavrin, L. Lipiäinen, K. Kokkonen, S. Novotny, M. Kaivola, and H. Ludvigsen, "Stroboscopic white-light interferometry of vibrating microstructures," Opt. Express **21**, 16901–16907 (2013).
2. L. Deck and P. de Groot, "High-speed non-contact profiler based on scanning white light interferometry," Appl. Opt. **33**, 7334–7338 (1994).
3. C. O'Mahony, M. Hill, M. Brunet, R. Duane, and A. Mathewson, "Characterization of micromechanical structures using white-light interferometry," Meas. Sci. Technol. **14**, 1807–1814 (2003).
4. T. Jo, K. Kim, S. Kim, and H. Pahk, "Thickness and surface measurement of transparent thin-film layers using white light scanning interferometry combined with reflectometry," J. Opt. Soc. Korea **18**, 236–243 (2014).
5. H. Gao, Y. Jiang, L. Zhang, and L. Jiang, "Five-step phase-shifting white-light interferometry for the measurement of fiber optic extrinsic Fabry–Perot interferometers," Appl. Opt. **57**, 1168–1173 (2018).
6. K. G. Larkin, "Efficient nonlinear algorithm for envelope detection in white light interferometry," J. Opt. Soc. Am. A **13**, 832–842 (1996).
7. S. Ma, C. Quan, R. Zhu, C. J. Tay, L. Chen, and Z. Gao, "Micro-profile measurement based on windowed Fourier transform in white-light scanning interferometry," Opt. Commun. **284**, 2488–2493 (2011).
8. S. Ma, C. Quan, R. Zhu, C. J. Tay, L. Chen, and Z. Gao, "Application of least-square estimation in white-light scanning interferometry," Opt. Laser Eng. **49**, 1012–1018 (2011).
9. P. De Groot and L. Deck, "Surface profiling by analysis of white-light interferograms in the spatial frequency domain," J. Mod. Opt. **42**, 389–401 (1995).
10. M. Li, C. Quan, and C. J. Tay, "Continuous wavelet transform for micro-component profile measurement using vertical scanning interferometry," Opt. Laser Technol. **40**, 920–929 (2008).
11. S. Chen, A. W. Palmer, K. T. V. Grattan, and B. T. Meggitt, "Digital signal-processing techniques for electronically scanned optical-fiber white-light interferometry," Appl. Opt. **31**, 6003–6010 (1992).
12. A. A. Chiayu and E. L. Novak, "Centroid approach for estimating modulation peak in broad-bandwidth interferometry," U.S. patent 5,633,715 (27 May 1997).
13. G. S. Kino and S. S. C. Chim, "Mirau correlation microscope," Appl. Opt. **29**, 3775–3783 (1990).
14. P. Pavliček and V. Michálek, "White-light interferometry—Envelope detection by Hilbert transform and influence of noise," Opt. Laser Eng. **50**, 1063–1068 (2012).
15. Q. Vo, F. Fang, X. Zhang, and H. Gao, "Surface recovery algorithm in white light interferometry based on combined white light phase shifting and fast Fourier transform algorithms," Appl. Opt. **56**, 8174–8185 (2017).
16. P. De Groot, "Principles of interference microscopy for the measurement of surface topography," Adv. Opt. Photonics **7**, 1–65 (2015).
17. I. Kiselev, V. Oberst, V. V. Sysoev, and U. Breitmeier, "A white-light interferometer as a gauge to measure the thickness of thin film: a practical extension of the phase method and correlogram summation," J. Opt. **17**, 125616 (2015).
18. P. De Groot, "Method and system for analyzing low-coherence interferometry signals for information about thin film structures," U.S. patent 7,564,566 (21 July 2009).
19. I. Kiselev, E. I. Kiselev, M. Drexel, and M. Hauptmannl, "Precision of evaluation methods in white light interferometry. Correlogram correlation method," Measurement **123**, 125–128 (2018).
20. Y. Zhou, H. Cai, L. Zhong, X. Qiu, J. Tian, and X. Lu, "Eliminating the influence of source spectrum of white light scanning interferometry through time-delay estimation algorithm," Opt. Commun. **391**, 1–8 (2017).
21. S. Debnath and M. Kothiyal, "Improved optical profiling using the spectral phase in spectrally resolved white-light interferometry," Appl. Opt. **45**, 6965–6972 (2006).
22. H. Altamar-Mercado, A. Patiño-Vanegas, and A. G. Marrugo, "Robust 3D surface recovery by applying a focus criterion in white light scanning interference microscopy," Appl. Opt. **58**, A101–A111 (2019).
23. P. De Groot, X. C. De Lega, R. Su, and R. Leach, "Does interferometry work?–A critical look at the foundations of interferometric surface topography measurement," Proc. SPIE **11102**, 11102–11115 (2019).